

DEM PARAMETERS CALIBRATION OF MIXED BIOMASS SAWDUST MODEL WITH MULTI-RESPONSE INDICATORS

混杂木屑离散元仿真模型的多响应参数标定

Gong Xun ¹⁾, Bai XueWei¹⁾, Huang HaiBo¹⁾, Zhang FengYu¹⁾, Gong YuanJuan¹⁾, Wei DeSheng²⁾

¹⁾Shenyang Agricultural University, College of Engineering, Shenyang / China;

²⁾Sunbon Agricultural Machinery Manufacturing Company, Siping / China

Tel: +86-024-88487117; E-mail: bai-xuewei@syau.edu.cn

DOI: <https://doi.org/10.35633/inmateh-65-19>

Keywords: mixed biomass sawdust, parameter calibration, DEM, constitutive property experiment

ABSTRACT

The Plackett-Burman factorial experiment was carried out by Design-Expert for 10 related factors. The simulation calibration experiment with JKR contact model was performed based on discrete element method (DEM) with mixed biomass sawdust as the research object. Taken the Box-Behnken experiment together with the steepest climbing test scheme, the parameters of the multi-response indicators were calibrated as follows: the Poisson's ratio of mixed biomass sawdust is 0.30; the density is 399.22kg·m⁻³; the recovery coefficient between sawdust particles is 0.47; the rolling friction coefficient between sawdust particles is 0.39 and the parameter of surface energy density between sawdust particles (JKR) is 0.29J·m⁻². The comparative verification experiments indicate that the relative error of the repose angle is 3.41% and the relative error of the stress-time response curve is less than 6.36%. These results verify the reliability of the calibration method and provide a theoretical reference for the study of the constitutive characteristics of biomass materials and the densification mechanism.

摘要

以混杂生物质木屑为研究对象，基于 DEM 离散元原理进行接触模型为 JKR 的仿真标定试验，利用 Design-Expert 针对 10 种相关因素进行 Plackett-Burman 析因试验，结合最陡爬坡试验方案，根据 Box-Behnken 试验，完成响应指标为堆积角、成型压制力、应力松弛时长的参数标定，其结果为：混杂木屑的泊松比 0.30，密度 399.22 kg·m⁻³，木屑颗粒间的恢复系数 0.47，木屑颗粒间的滚动摩擦系数 0.39，木屑颗粒间的 JKR 表面能密度 0.29 J·m⁻²。通过对比验证试验可知，堆积角的相对误差为 3.41%，应力-时间响应曲线的相对误差小于 6.36%，验证了该标定方法的可靠性，为生物质本构特性及致密成型机理的研究提供了理论参考。

INTRODUCTION

Mixed biomass sawdust is identified as a substitute of fossil energy for its inflammability, low ash content, low sulfur content, and high calorific value. Constitutive parameters of mixed biomass sawdust are of great significance for the development of pelleting machines (Chen *et al.*, 2020). Due to the wide divergence in the composition and morphology, and the high nonlinearity versus heterogeneity of the contact between components of sawdust, it is difficult to measure the mechanical constitutive parameters directly. Based on the dynamic relaxation theory, the discrete element method which analyzes integral subjects through discrete elements and takes Newton's second law as the basic theory, the parameters of nonlinearity materials by simplifying the material to particles can be calibrated. Therefore, the analysis method based on DEM is introduced to calibrate the constitutive parameters of mixed biomass sawdust (Liu *et al.*, 2019).

As reported, the parameters of mixed biomass sawdust which were calibrated by discrete element method are various. The values selected by different scholars are also quite different even on the same type of specimens of mixed biomass sawdust. Therefore, it is necessary to recalibrate the discrete element parameters of mixed biomass sawdust (Li *et al.*, 2019).

Recently, Horabik *et al.* calibrated the parameters of wheat particles by using the double stiffness Hertz contact model based on the DEM. The Poisson's ratio, the rolling friction coefficient, and the recovery coefficient are 0.25, 0.01, and 0.5 respectively, and the calibration error compared with physical experiment is 0.57% (Horabik *et al.*, 2020). Mostafa *et al.* calibrated the parameters of soil based on the discrete element principle combined with the contact model of hysteresis spring and linear cohesion (HS-LC).

The Poisson's ratio, the recovery coefficient, and the dynamic friction coefficient are 0.3, 0.6, and 0.5 respectively (Mostafa *et al.*, 2020). Kornél *et al.* calibrated the parameters of rapeseed based on the discrete element principle and uniaxial compression experiment. The results showed that the friction coefficient between particles is 0.5 and the local damping coefficient is 0.7 (Kornél *et al.*, 2015). Zhang *et al.* investigated and calibrated 15 factors including JKR parameter by referring to the data of concrete slump experiment. Using the accumulation height as the responding index combined with the analysis principle of discrete element, it was found that the static friction coefficient is 0.36, the rolling friction coefficient is 0.09 and the JKR parameter is $6.69\text{J}\cdot\text{m}^{-2}$ (Zhang *et al.*, 2020). Zhang *et al.* calibrated the parameters of blueberries by Plackett-Burman factorial experiment and central experiment with the angle of repose as responding index through discrete element simulation analysis. The results showed that the recovery coefficient is 0.06, the static friction coefficient is 0.56, the angle of repose is 24.66° , and the calibration error is 0.57% (Zhang *et al.*, 2020).

Extending from the above literatures, the parameters of response target in this study not only used repose angle as the single target value, but also included compaction force and stress relaxation time. Design-Expert was applied to investigate the Poisson's ratio, JKR parameter and other 10 factors based on Plackett-Burman factorial experiment, steepest ascent experiment and Box-Behnken experiment. The repose angle, molding compaction force and stress relaxation time were used as the response indicators in these experiments. Using the Hertz-Mindlin with JKR contact theory, combined with the DEM simulation analysis method, the Poisson's ratio, density, inter-particle recovery coefficient, inter-particle rolling friction coefficient and JKR parameter were calibrated for the mixed biomass sawdust.

MATERIALS AND METHODS

Materials

The mixed biomass sawdust of eucalyptus, arbores and other industrial production surplus was selected in this work. Sawdust samples of 200g were processed by screening out of stones and other industrial impurities by vibration sieve, according to the standard 'particle size distribution (GB / T14684 - 2001)'. The sawdust sample is gradually screened by standard test sieve. The size range of particle sample is shown in Table 1.

Table 1

Grading of sawdust particles	
Particle size /mm	Proportion /%
≤0.15	7.53
0.15~0.18	6.12
0.18~0.25	8.57
0.25~0.45	7.74
0.45~0.60	7.62
0.60~0.90	15.68
0.90~2.00	35.21
2.00≥	11.53
Total	100

According to the standard "Determination of moisture content of forestry biomass materials (GB/T36055-2018)", the moisture content of sawdust samples without impurities was determined. Random sawdust sample of 2.00g was weighed, put in a $(105\pm 2)^\circ\text{C}$ oven and weighed again after drying. Parallel tests were repeated in 8 groups, and the average moisture content of sawdust samples is $(8.5\pm 0.3)\%$.

Method

The parameters of mixed biomass sawdust were calibrated by simulation experiment and physical experiment. First, the repose angle of mixed biomass sawdust was measured, and then the stress-time response curve was obtained by single-mode hole compression experiment.

According to the Plackett-Burman factorial experiment, the factors with significant influence are selected from 10 related factors such as JKR and Poisson's ratio. Ultimately, the steepest ascent experiment was used to determine the optimal value range along the gradient direction of the response surface, and the variance analysis in the Box-Behnken experiment was used to optimize the target factors and to complete the parameter calibration of the related variables.

Measurement of mixed biomass sawdust repose angle

According to the measurement of the repose angle in the standard '(GB/T31057.2-2018) particle material physical properties experiment', the repose angle of mixed biomass sawdust was measured as shown in Fig.1, where the funnel taper is $60\pm 0.5^\circ$ and the outlet diameter is 10mm. The distance between the flow outlet surface and the tray surface is 80 ± 2 mm. The camera and the material tray plane were adjusted to the same level, photographed when the steady-state repose angle formed. Then, 20g mixed biomass sawdust samples were randomly weighed and used for the experiments. The parallel experiments were repeated for 5 times.



Fig. 1 - Measurement test of the repose angle of mixed biomass sawdust

As shown in Fig.2, the background was eliminated by using the method of image recognition, and it was transformed into a binary image and the contour of the repose angle was extracted. The angle between the fitted straight line and the horizontal plane is the repose angle. The average of repose angles obtained by five groups of parallel experiments is $32.40\pm 0.2^\circ$ (Peilin et al., 2020).

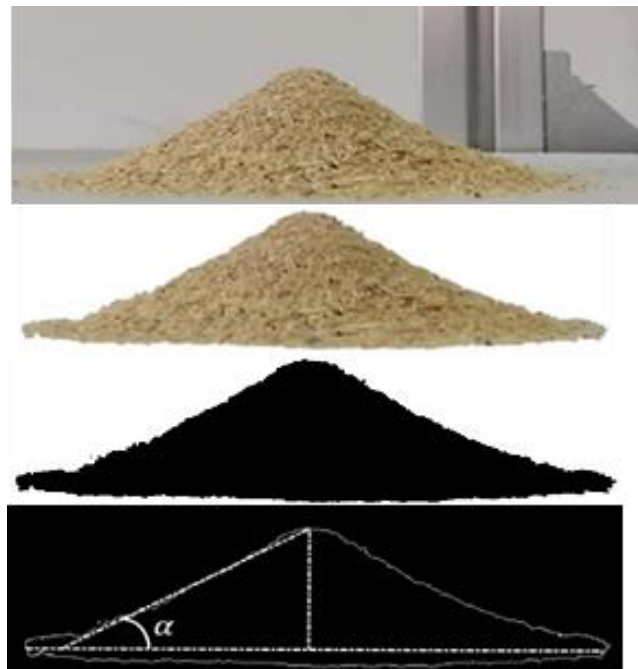


Fig. 2 - Image processing of repose angle

Compacting experiment of mixed biomass sawdust

As shown in Fig.3, the material of the mold is PLA which is produced by 3D-Printer. The compacting experiment was carried out by WDW-100A universal test bench.

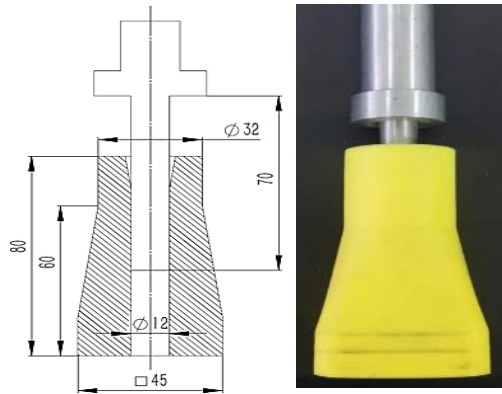


Fig. 3 - Forming test mold

Before compacting, the bottom surface of the pressing rod was aligned with the upper end of the mold, and the displacement count of the equipment was set to zero. At the beginning of compacting, the pressing rod was compressed downward at the speed of 15.00mm·s⁻¹ and stopped at 30.00mm. The current position was maintained for 60.00 s. During this period, the material entered the stress relaxation stage. Four groups of parallel tests were carried out and it was found that the average compacting force was 1436.30N and the average stress relaxation time was 43.60 s. The compressed pellets bar is shown in Fig.4.



Fig.4 - Compressed pellets bar

SIMULATION ANALYSIS BASED ON DISCRETE ELEMENT METHOD

Selection of contact model

In order to express the surface energy of particles, Hertz-Mindlin with JKR theory established the relationship between the normal elastic force, normal overlap and surface energy of the contact particles, reflecting the viscoelasticity and mechanical properties of particles, as Eq. (1-2):

$$F_{JKR} = -4\sqrt{\pi\gamma E^*} \alpha^{\frac{3}{2}} + \frac{4E^*}{3R^*} \alpha^3 \tag{1}$$

$$\delta = \frac{\alpha^*}{R^*} - \sqrt{\frac{4\pi\gamma\alpha}{E^*}} \tag{2}$$

where: F_{JKR} represents the normal elastic force of contact, γ represents the particle surface energy, E^* represents the equivalent elastic modulus, α represents the surface contact radius between particles, R^* represents the equivalent contact radius of particles, δ represents the normal overlap between particles.

The equivalent elastic modulus and contact radius can be obtained by the contact radius and Poisson's ratio of two contact particles as Eq. (3-4):

$$\frac{1}{E^*} = \frac{1-\nu_1^2}{E_1} + \frac{1-\nu_2^2}{E_2} \tag{3}$$

$$\frac{1}{R^*} = \frac{1}{R_1} + \frac{1}{R_2} \tag{4}$$

where: ν represents the Poisson's ratio of particles.

Hertz-Mindlin with JKR theory can show the mechanical properties of viscoelastic particles, so this contact model is selected for simulation test (*Johnson et al., 1971; Mahdi et al., 2020*).

Construction of simulation model and parameter setting

According to the screening results of mixed biomass sawdust, spherical particles with different sizes were created in the pre-processing module of EDEM. Six sections were created in size distribution module and set to the particle size range obtained by screening experiment. The funnel was created by geometries module. The inclination angle of the inner wall of the funnel is 60° , and the diameter of the outlet at the lower end is 10.00mm which is 80.00mm away from the horizontal plane. The Poisson's ratio of the model material is set to 0.3, the density is set to $7870.00 \text{ kg}\cdot\text{m}^{-3}$, and the shear modulus is $8.17 \times 10^7 \text{ MPa}$. The attribute parameters of the particles are set according to the factor values of the subsequent Plackett-Burman and Box-Behnken experiments.

The Hertz-Mindlin with JKR model was selected as the contact model, and the gravity acceleration is set to $9.81 \text{ m}\cdot\text{s}^{-2}$, and the direction is vertical downward. Ultimately, the analysis module was imported and set Rayleigh time step at 20%, the total simulation time at 10s, and the grid radius to three times of minimum radius. The simulation analysis process is shown in Fig.5 (Hao et al., 2020; Seunghyun et al., 2019).



Fig. 5 - Simulation test of repose angle

Referring to the experimental results according to compacting of mixed biomass sawdust, the compression model was created in the geometries module of EDEM as shown in Fig.6, and the speed of the compression plane was set to $15 \text{ mm}\cdot\text{s}^{-1}$, and the total time was set to 60s for simulation analysis (Hamid et al., 2020).

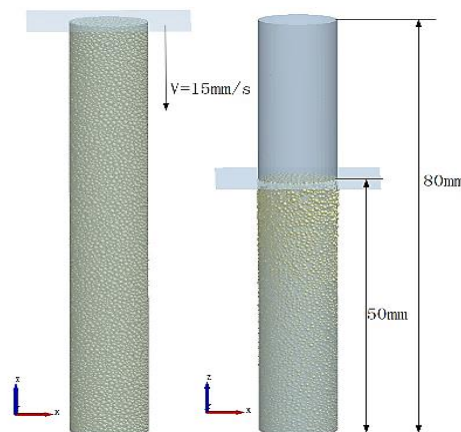


Fig. 6 - Simulation test of single-mode hole compacting

RESULTS

Plackett-Burman factorial experiment

Based on the requirements of Plackett-Burman factorial experiment, 10 variables including Poisson's ratio of mixed biomass sawdust, shear modulus, density, inter-particle recovery coefficient, inter-particle static friction coefficient, inter-particle rolling friction coefficient, inter-particle recovery coefficient with mold inner wall, inter-particle static friction coefficient with mold inner wall, inter-particle rolling friction coefficient with mold inner wall, and JKR parameter are selected for factor significance screening.

Due to the data of discrete element simulation models are quite different, therefore the range of above factors is determined according to the material library of EDEM and relevant papers. As shown in Table 2, the Poisson's ratio range of mixed biomass sawdust was found to be 0.1-0.5, the shear modulus range to be 1-10MPa, the particle density range to be 300-500kg·m⁻³, the recovery coefficient between particles to be 0.1-0.8, the static friction coefficient between particles to be 0.01-0.8, the rolling friction coefficient between particles to be 0.01-0.8, the recovery coefficient between sawdust and mold inner wall to be 0.1-0.8, the static friction coefficient between sawdust and mold inner wall to be 0.01-0.8, the rolling friction coefficient between sawdust and mold inner wall to be 0.01-0.8, and the JKR parameter is 0.05-0.5J·m⁻².

Table 2

Plackett-Burman test factor level table

Factor symbols	Factors	Factor levels		
		-1	0	1
T1	Poisson's ratio between particles	0.10	0.30	0.50
T2	Shear modulus between particles / MPa	1.00	5.50	10.00
T3	Particles density / kg·m ⁻³	300.00	400.00	500.00
T4	Recovery coefficient between particles	0.10	0.45	0.80
T5	Coefficient of static friction between particles	0.01	0.41	0.80
T6	Coefficient of rolling friction between particles	0.01	0.41	0.80
T7	Restoring coefficient with mold inner wall	0.10	0.45	0.80
T8	Static friction coefficient with mold inner wall	0.01	0.41	0.80
T9	Rolling friction coefficient with mold inner wall	0.01	0.41	0.80
T10	Parameter of surface energy density between particles (JKR) /J·m ⁻²	0.05	0.28	0.50

According to the factor level determined in table 2, factorial tests were carried out as shown in table 3, where T11 is an empty column; index Y1 is the repose angle; index Y2 is the molding pressing force (i.e., the peak stress of the compression plane at the end of compression); and index Y3 is the duration of stress relaxation (i.e., the duration of stress relaxation when the compression plane stops moving to 0).

Table 3

Plackett-Burman simulation test

Run No.	T1	T2	T3	T4	T5	T6	T7	T8	T9	T10	T11	Y1/°	Y2/N	Y3/s
1	1	1	1	-1	-1	-1	1	-1	1	1	-1	24.37	1402.63	39.18
2	1	1	-1	1	1	1	-1	-1	-1	1	-1	48.56	1536.84	41.21
3	1	-1	1	1	-1	1	1	1	-1	-1	-1	35.41	1237.87	45.32
4	1	-1	1	1	1	-1	-1	-1	1	-1	1	13.98	1168.94	29.73
5	-1	1	-1	1	1	-1	1	1	1	-1	-1	30.06	1654.31	19.13
6	-1	-1	1	-1	1	1	-1	1	1	1	-1	21.92	1099.36	16.36
7	1	-1	-1	-1	1	-1	1	1	-1	1	1	42.65	1264.82	20.96
8	-1	1	1	-1	1	1	1	-1	-1	-1	1	19.96	1374.98	22.98
9	-1	1	1	1	-1	-1	-1	1	-1	1	1	28.12	1498.11	48.54
10	-1	-1	-1	-1	-1	-1	-1	-1	-1	-1	-1	17.11	964.37	55.44
11	-1	-1	-1	1	-1	1	1	-1	1	1	1	32.49	953.22	65.71
12	1	1	-1	-1	-1	1	-1	1	1	-1	1	38.52	1934.76	14.65

Through the analysis on the experimental results of the response index as the repose angle shown in Table 4, the R² value adjusted by the model was 0.9978 with P value less than 0.05, suggesting the model is statistically validated for further analysis. The observation shows that the factors T1, T3, T6 and T10 are extremely significant; T2 and T4 are significant; and T1, T2, T4, T6 and T10 have positive effects on the repose angle, indicating the repose angle increases with the increase of the factor. The factor T3 has a negative effect on the repose angle, suggesting the repose angle decreases with the increase of the factor. Among them, T3, T1 and T10 have greater contributions to the repose angle results, while T2 and T4 have smaller contributions to the repose angle results. Similarly, the model is justified again by the R² value to be 0.9906 with the P value as 0.0625 when the response index is the molding compaction force. Factors T3 and T4 are extremely significant, while T1, T6, T10 and T8 are significant. Only factors T3, T10 had a negative effect on the molding force. By analyzing the test that the response index to be the stress relaxation time, the model demonstrated statistical significance with R² value adjusted by the model to be 0.9989 and the P value to be 0.0178.

Factors T10, T4 and T3 are extremely significant; T1, T6 and T5 are significant; only factors T10 and T4 had positive effect on stress relaxation time. In summary, T1, T3, T4, T6 and T10 are selected as the factors that have significant effects on indicators Y1, Y2 and Y3, and they are used as the factors for subsequent experimental investigations.

Table 4

Plackett-Burman simulation test analysis

Factors	Standardized effects	Contribution degree/%	Sum of mean squares	F-value	P-value
Model			1232.52	505.82	0.03**
T1	8.97	19.59	241.47	990.96	0.02**
T2	4.34	4.58	56.46	231.72	0.05*
T3	-10.94	29.12	358.94	1473.03	0.01**
T4	4.02	3.92	48.36	198.46	0.06*
T5	0.19	0.02	0.11	0.42	0.63
T6	6.76	11.13	137.16	562.89	0.02**
T7	2.79	1.89	23.32	0.72	0.56
T8	6.71	10.93	134.74	1.94	0.22
T9	-5.08	6.28	77.37	0.81	0.43
T10	7.18	12.54	154.59	634.39	0.02**

Note: $p \leq 0.05$ is extremely significant, expressed as "***"; $0.05 \leq p \leq 0.1$ is significant, expressed as "**"

Steepest ascent experiment

As shown in table 5, the significant factors filtered by Plackett-Burman are increased or decreased according to a certain step length, and the optimal range is determined according to the positive and negative effects of relative errors of each response index. The analysis shows that the repose angle index is bounded by the No.4 test, and the relative error decreases first and then increases. The compacting force index is bounded by the No.3 test, and its relative error decreases first and then increases. The stress relaxation time index is bounded by the No.4 test, and the relative error decreases first and then increases. Therefore, it is appropriate to select the values of the factors corresponding to experiment No.2 as the lower limit, and the values of the factors corresponding to experiment No.5 as the upper limit for Box-Behnken experiment, namely, T1 to be 0.18–0.42, T3 to be 340–460, T4 to be 0.24–0.66, T6 to be 0.17–0.62, and T10 to be 0.14–0.41.

Table 5

Analysis of the steepest ascent test

Run No.	Factors					Y1 relative error	Y2 relative error	Y3 relative error
	T1	T3	T4	T6	T10			
1	0.10	300	0.10	0.01	0.05	42.24%	33.83%	31.71%
2	0.18	340	0.24	0.17	0.14	37.11%	12.51%	25.63%
3	0.26	380	0.38	0.32	0.23	15.37%	4.72%	18.42%
4	0.34	420	0.52	0.47	0.32	9.23%	17.64%	5.14%
5	0.42	460	0.66	0.62	0.41	22.61%	29.76%	13.35%
6	0.50	500	0.80	0.80	0.50	38.12%	35.13%	27.84%

Calibration of simulation parameters and validation test

According to the factor value range of the steepest ascent experiment, 46 groups of Box-Behnken experiments including 6 groups of central experiments were carried out (Boikov et al., 2019). Through the analysis of the test with the repose angle as the index, the P value is found to be extremely significant at 0.012 with the adjusted R^2 value at 0.9954. However, the P value of the mismatch term is not significant at 0.2663, indicating that the model is well fitted. By analyzing the compacting force as the index of the test, the P value is significantly 0.0634 with the adjusted R^2 value at 0.9824, and the P value of the mismatch item at 0.1817 is not significant, indicating that the model is well fitted. The analysis of the test with compacting force as the index shows that the P value is extremely significant at 0.0156; the adjusted R^2 value is 0.9934; and the P value of the unfit term is not significant at 0.2216, indicating that the model is well fitted. Multi-objective optimization of the regression model is carried out by taking the repose angle of 32.4°, compacting force of 1436.3N, and stress relaxation time of 43.6s as the appropriate values.

The analysis shows that when the Poisson's ratio of mixed biomass sawdust is 0.30; the density is $399.22 \text{ kg}\cdot\text{m}^{-3}$; the recovery coefficient between particles is 0.47; the rolling friction coefficient between particles is 0.39, and the JKR parameter is $0.29 \text{ J}\cdot\text{m}^{-2}$, demonstrating that the response index is the most approach to the target value.



Fig. 7 - Comparison with simulation and physical experiment of repose angle

The calibrated parameters are imported into EDEM to carry out the single-hole compression simulation test as described above. The simulated data of stress versus time is plotted in the same coordinated system with the test data. Time duration is 45s, and the total number of data points investigated is 2000 as shown in Fig.8.

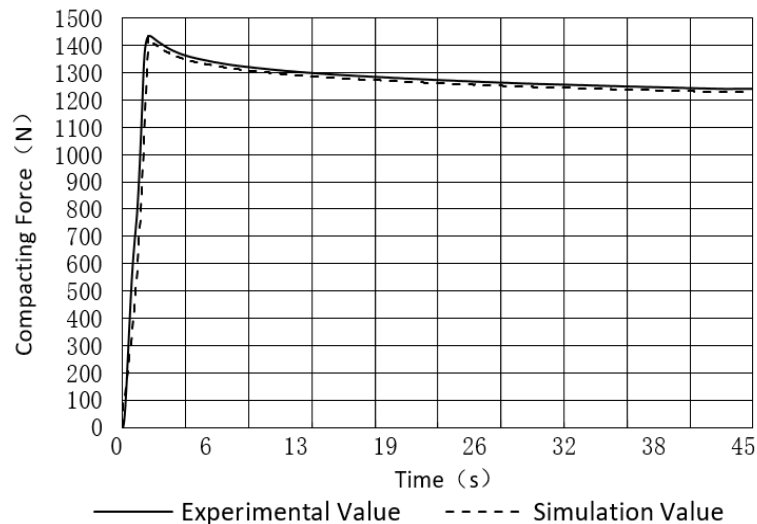


Fig. 8- Simulation versus experiment force data on time

The result shows that the maximum relative error between the actual value and the simulation value in the compacting process is 6.36%. By comparing with the compacting stage before the peak value of the pressing force and the stress relaxation stage after the peak value, it shows that the average relative error of the former is generally greater than that of the latter. This can be explained that the simulation test environment is ideal, and the compression mold inner wall does not affect each other, however, the actual test environment is relatively complicated. There is friction between the outer surface of the pressure rod and the inner wall of the mold, and there are differences in surface roughness between them. Therefore, friction is a variable with time. Once the influence of friction is eliminated when the movement of pressure rod stops and is in the stress relaxation stage, the fitting degree of the stress relaxation stage curve is the best.

CONCLUSIONS

(1) The mixed biomass sawdust of industrial surplus in the experiment shows the wet base moisture content at 8.50%, particle size less than or equal to 2mm, repose angle at 32.40° , compacting pressure to be 1436.30N, and the stress relaxation time to be 43.60s. Combined with the analysis method of discrete element method, the Hertz-Mindlin with JKR is used as the contact model, and the simulation analysis is carried out.

(2) Through the Plackett-Burman factorial experiment, ten factors including Poisson's ratio of mixed biomass sawdust, shear modulus, density, inter-particle recovery coefficient, inter-particle static friction

coefficient, inter-particle rolling friction coefficient, inter-particle recovery coefficient with mold inner wall, inter-particle static friction coefficient with mold inner wall, inter-particle rolling friction coefficient with mold inner wall, and JKR parameter are investigated. The factors that have significant effects on repose angle, compacting force and stress relaxation time are screened as follows: Poisson's ratio of mixed biomass sawdust, density, inter-particle recovery coefficient, inter-particle rolling friction coefficient, and JKR parameter.

(3) The steepest ascent test was used to determine the optimal range of target factors, and the multi-objective optimization was carried out through the Box-Behnken test with the repose angle of 32.40°, compacting pressure of 1436.30N and stress relaxation time of 43.60s. The obtained calibration parameters are as follows: the Poisson's ratio of mixed biomass sawdust to be 0.30, the density to be 399.22kg·m⁻³, the recovery coefficient between particles to be 0.47, the rolling friction coefficient between particles to be 0.39, and the JKR parameter to be 0.29J·m⁻².

(4) The calibrated parameters are compared with the results of the actual test. The relative error of the repose angle is 3.41%, and the maximum relative error of the stress-time response curve is less than 6.36%.

ACKNOWLEDGEMENT

The experimental equipment and experimental sites of this study are provided by Shenyang Agricultural University. The authors want to thank associate professor Xuwei Bai, Professor Yuanjuan Gong and Professor Yongkui Li for their academic guidance. Thanks also goes to Doctor Shuo Qiu in the laboratory for the technical support to this research. The authors gratefully acknowledge the financial support provided by Liaoning Provincial Education Department Fund (LSNQN201904) and Natural Science Foundation of China (51405311).

REFERENCES

- [1] Boikov A.V., Savelev R.V., Payor V.A. et al., (2019), DEM calibration approach: orthogonal experiment. *The Journal of Physics: Conference Series*. vol. 1210(1), Russia. <https://iopscience.iop.org/article/10.1088/1742-6596/1210/1/012025>
- [2] Chen G.Q., Yan J.X. et al., (2020), Simulation study on accumulation characteristics of maize particles by discrete element method (玉米颗粒堆积特性的离散元法模拟研究), *The Journal of light Industry Mechanics*. vol. 38(06), pp.11-14, Jiangsu/China. <https://kns.cnki.net/KCMS/detail/detail.aspx?dbcode=CJFD&filename=QGJX202006003>
- [3] Hamid Gilvari, Wiebren de Jong, Dingena L. Schott, (2020), Breakage behavior of biomass pellets: an experimental and numerical study. *The Journal of Computational Particle Mechanics*. vol.2020, pp. 1-14, Netherlands. <https://link.springer.com/article/10.1007/s40571-020-00352-3>
- [4] Hao Chen, Shiwei Zhao, Xiaowen Zhou, (2020), DEM investigation of angle of repose for super-ellipsoidal particles. *The Journal of Particuology*. vol. 50, pp. 53-66, China. <https://www.sciencedirect.com/science/article/abs/pii/S1674200119300975>
- [5] Horabik J., Wiącek J., Parafiniuk P. et al., (2020), Calibration of discrete-element-method model parameters of bulk wheat for storage, *The Journal of Biosystems Engineering*. vol.200, pp. 298-314, Lublin/Poland. <https://www.sciencedirect.com/science/article/pii/S1537511020302889>
- [6] Johnson K.L., Kendall K., Robert A.D., (1971), Surface energy and contact of elastic solids, *The Journal of Proceedings of the Royal Society of London*. vol.324, pp.301-313, United Kingdom. <https://royalsocietypublishing.org/doi/abs/10.1098/rspa.1971.0141>
- [7] Kornél Tamás, Bernát Földesi, János Péter Rádics et al., (2015), A Simulation Model for Determining the Mechanical Properties of Rapeseed using the Discrete Element Method, *The Journal of Periodica Polytechnica Civil Engineering*. vol. 59(4), pp. 575-582, Hungary. http://www.onacademic.com/detail/journal_1000041692106299_f7d4.html
- [8] Liu X.T., Gao Y.H. et al., (2019), Discrete element analysis of raw material geometry in biomass compacting process (生物质致密成型过程中原料几何形状的离散元研究), *The Journal of China Agricultural Machinery Chemistry*. vol. 40(09), pp.80-84, Baotou/China. https://kns.cnki.net/kcms/detail/detail.aspx?dbcode=CJFD&dbname=CJFDLAST2019&filename=GLJH201909015&uniplatform=NZKPT&v=0IRR2JQ23ZFrMOBo6EE-qBTj1j--a09p5x80cZb80tx1E-UM_6ljFqG3TGGYXe3g

- [9] Li Z. et al., (2019), Discrete element study on force chain evolution in densification process of Salix fine branch particles (沙柳细枝颗粒致密成型过程中力链演变的离散元研究), *The Journal of Acta Energiæ Solaris Sinica*. vol. 40(11), pp.3186-3195, Baotou/China.
<https://kns.cnki.net/kcms/detail/detail.aspx?dbcode=CJFD&dbname=CJFDLAST2019&filename=TYLX201911023&uniplatform=NZKPT&v=cOC7fu0rsHQE5ScNMEVeD6CapW6IDqYsnAOt6EJGrSfC0vEBDxVwgA7ju32YUSAg>
- [10] Mahdi Joulaei, Mojtaba Kolahdoozan, Mehdi Salehi, et al., (2020), Comparison of the adhesion forces in single and double layer coatings on the MEMS surfaces by JKR and DMT models. *The Journal of Surface and Interface Analysis*. vol. 52(1-2), pp. 34-41, Iran.
<https://analyticalsciencejournals.onlinelibrary.wiley.com/doi/full/10.1002/sia.6719>
- [11] Mostafa Bahrami, Mojtaba Naderi Boldaji, Davoud Ghanbarian et al., (2020), Simulation of plate sinkage in soil using discrete element modelling: Calibration of model parameters and experimental validation, *The Journal of Soil and Tillage Research*. vol. 203, Iran.
<https://www.sciencedirect.com/science/article/pii/S0167198720304827>
- [12] Peilin Li, Mustafa Ucgul, Sang-Heon Lee et al., (2020), A new approach for the automatic measurement of the angle of repose of granular materials with maximal least square using digital image processing, *The Journal of Computers and Electronics in Agriculture*. vol.172, Australia.
<https://www.sciencedirect.com/science/article/pii/S016816991932438X>
- [13] Seunghyun Lee, Junyoung Park., (2019), Standardized Friction Experiment for Parameter Determination of Discrete Element Method and Its Validation Using Angle of Repose and Hopper Discharge. 2019, *The Journal of Multiscale Science and Engineering*. vol. 1(3), pp. 247-255, Korea.
<https://link.springer.com/article/10.1007/s42493-019-00020-6>
- [14] Zhang K. et al., (2020), Parameter calibration of concrete discrete element based on JKR bond model (基于 JKR 黏结模型的混凝土离散元参数标定), *The Journal of Concrete*. vol. 2020(08), pp.46-50+55, Liaoning/China.
<https://kns.cnki.net/kcms/detail/detail.aspx?dbcode=CJFD&dbname=CJFDLAST2020&filename=HLTF202008012&uniplatform=NZKPT&v=RplydeDh1a7BjxRWjCfjpHw8O4eVUV08JuJBWE Ln-52eVMcXrMKUUoBX-8wXhwQY>
- [15] Zhang L.W. et al., (2020), Parameter calibration of blueberry discrete element based on response surface method (基于响应面法的蓝莓离散元参数标定), *The Journal of Shenyang Agricultural University*. Vol.51(05), pp. 540-548, Liaoning/China.
https://kns.cnki.net/kcms/detail/detail.aspx?dbcode=CJFD&dbname=CJFDLAST2020&filename=SYNY202005005&uniplatform=NZKPT&v=bd3CB3KQFIYcXn6_k_cVd2giaZcERycTHq3pj8o7eviOnex9_kl QndgIKdNYRkn2